Published in final edited form as:
J Mol Cell Cardiol. 2010 November ; 49(5): 746–752. doi:10.1016/j.yjmcc.2010.08.013.

HIV protease inhibitors elicit volume-sensitive Cl^- current in cardiac myocytes via mitochondrial ROS

Wu Deng[a], **Lia Baki**[a], **Jun Yin**[b], **Huiping Zhou**[c], and **Clive M. Baumgarten**[a,b,*]

[a] Department of Physiology and Biophysics, Medical College of Virginia, Virginia Commonwealth University, Richmond, VA 23298 USA

[b] Departments of Internal Medicine (Cardiology), Virginia Commonwealth University, Richmond, VA 23298 USA

[c] Department of Microbiology and Immunology, Virginia Commonwealth University, Richmond, VA 23298 USA

Abstract

HIV protease inhibitors (HIV PI) reduce morbidity and mortality of HIV infection but cause multiple untoward effects. Because certain HIV PI evoke production of reactive oxygen species (ROS) and volume-sensitive Cl^- current ($I_{Cl,swell}$) is activated by ROS, we tested whether HIV PI stimulate $I_{Cl,swell}$ in ventricular myocytes. Ritonavir and lopinavir elicited outwardly-rectifying Cl^- currents under isosmotic conditions that were abolished by the selective $I_{Cl,swell}$-blocker DCPIB. In contrast, amprenavir, nelfinavir, and raltegravir, an integrase inhibitor, did not modulate $I_{Cl,swell}$ acutely. Ritonavir also reduced action potential duration, but amprenavir did not. $I_{Cl,swell}$ activation was attributed to ROS because ebselen, an H_2O_2, scavenger, suppressed ritonavir- and lopinavir-induced $I_{Cl,swell}$. Major ROS sources in cardiomyocytes are sarcolemmal NADPH oxidase and mitochondria. The specific NADPH oxidase inhibitor apocynin failed to block ritonavir- or lopinavir-induced currents, although it blocks $I_{Cl,swell}$ elicited by osmotic swelling or stretch. In contrast, rotenone, a mitochondrial e^- transport inhibitor, suppressed both ritonavir- and lopinavir-induced $I_{Cl,swell}$. ROS production was measured in HL-1 cardiomyocytes with C-H_2DCFDA-AM and mitochondrial membrane potential ($\Delta\Psi_m$) with JC-1. Flow cytometry confirmed that ritonavir and lopinavir but not amprenavir, nelfinavir, or raltegravir augmented ROS production, and HIV PI-induced ROS production was suppressed by rotenone but not NADPH oxidase blockade. Moreover, ritonavir, but not amprenavir, depolarized $\Delta\Psi_m$. These data suggest ritonavir and lopinavir activated $I_{Cl,swell}$ via mitochondrial ROS production that was independent of NADPH oxidase. ROS-dependent modulation of $I_{Cl,swell}$ and other ion channels by HIV PI may contribute to some of their actions in heart and perhaps other tissues.

Keywords

$I_{Cl,swell}$; VRAC; HIV protease inhibitors; reactive oxygen species; mitochondria; mitochondrial membrane potential; NADPH oxidase; swelling; cell volume

* Corresponding author: Clive M. Baumgarten, Ph.D., Dept. of Physiology & Biophysics, Virginia Commonwealth Univ., 1101 E. Marshall St., Richmond, VA 23298-0551 USA, Tel.: +1 804 828 4773, Fax: +1 804 828 7382, clive.baumgarten@vcu.edu.

Disclosures: None

1. Introduction

Inclusion of HIV protease inhibitors (HIV PI)[1] in highly active anti-retroviral therapy substantially reduces the morbidity and mortality of HIV infections. A significant challenge is their adverse effects, which include hyperlipidemia, lipodystrophy, insulin resistance, and increased risks of atherosclerosis and myocardial infarction (for review, see [1]). Arrhythmogenic effects also are reported. HIV PI cause PR and QT_c prolongation and torsade de pointes in patients [2-4] and suppress heterologously expressed hERG currents and I_{Kr} in ventricular myocytes [2]. Moreover, HIV PI cause endothelial cell damage [5] and decompensated heart failure [6] in experimental settings, and dilated cardiomyopathy and heart block in human neonates [7].

Recent studies indicate that HIV PI augment production of reactive oxygen species (ROS) in the vasculature [8-12], adipocytes [13,14], macrophage-derived foam cells [15], fibroblast [16], and pancreatic β cells [17], suggesting that oxidative stress may play a role in the adverse effects of HIV PI. HIV PI reduce mitochondrial membrane potential, which triggers mitochondrial ROS production [11,15], and the expression of mitochondrial respiratory chain proteins is diminished [16,18]. Moreover, expression of NADPH oxidase subunit mRNAs is augmented [15].

We hypothesize that HIV PI-induced ROS production modulates ion channel function and, thereby, may contribute to untoward effects in heart and perhaps other tissues. One potential target is the outwardly rectifying, volume- and stretch-sensitive Cl^- current, $I_{Cl,swell}$. We previously demonstrated that activation of ROS production by osmotic swelling, stretch, and downstream signaling proteins, as well as exogenous H_2O_2, elicit $I_{Cl,swell}$ in ventricular myocytes [19-21]. ROS-induced $I_{Cl,swell}$ activation also was identified in HeLa and HTC hematoma cell lines [22,23] and primary astrocytes [24]. These studies concluded that ROS production by NADPH oxidase is a required intermediate that elicits $I_{Cl,swell}$, and we recently found mitochondrial ROS also is necessary [25].

We tested whether HIV PI elicit $I_{Cl,swell}$ in cardiomyocytes and identified the source of ROS. Under isosmotic conditions, clinically relevant concentrations of the HIV PI ritonavir (RTV) and lopinavir (LPV) rapidly induced an outwardly-rectifying Cl^- current, and RTV decreased action potential duration (APD) by 60 ms, effects that were fully blocked by the $I_{Cl,swell}$ inhibitor DCPIB. HIV PI-induced $I_{Cl,swell}$ also was blocked by the ROS scavenger ebselen and by rotenone, which inhibits mitochondrial e^- transport. In contrast, the NADPH oxidase inhibitor apocynin had no effect. Furthermore, the HIV PI inhibitors amprenavir (APV) and nelfinavir (NFV) and the HIV integrase inhibitor raltegravir (MK-0518) failed to acutely modulate $I_{Cl,swell}$, and APV failed to alter APD. Flow cytometry confirmed that RTV and LPV, but not APV, NFV or MK-0518, augmented ROS production measured in HL-1 myocytes. As found for $I_{Cl,swell}$, HIV PI-induced ROS production was inhibited by rotenone but not by suppressing NADPH oxidase activity. Additionally, RTV, but not APV, depolarized mitochondrial membrane potential, $\Delta\Psi_m$. These data suggest that RTV and LPV acutely activated $I_{Cl,swell}$ via mitochondrial ROS production, most likely at complex III, and that ROS arising from NADPH oxidase were not required.

[1]***Abbreviations:*** APD, action potential duration; DNP, 2,4-dinitrophenol; HIV PI, HIV protease inhibitors; ROS, reactive oxygen species; $I_{Cl,swell}$, volume- sensitive Cl^- current; $\Delta\Psi_m$, mitochondrial membrane potential; RTV, ritonavir; LPV, lopinavir; APV, amprenavir; NFV, nelfinavir; and MK-0518, raltegravir.

2. Materials and methods

Detailed methods are given in the Online Supplement. Animal studies were approved by the Institutional Animal Care and Use Committee and were conducted in accordance with the Declaration of Helsinki, and the *Guide for the Care and Use of Animals* (National Academy Press, Washington, D.C., 1996).

Ventricular myocytes for electrophysiological studies were freshly isolated from anesthetized New Zealand white rabbits (~3 kg) by enzymatic digestion. HL-1 cardiomyocytes were used for flow cytometry because they provide a more homogeneous population than freshly isolated myocytes, which unavoidably included damaged cells.

2.1. Electrophysiology

Recordings were made at room temperature with fire-polished pipettes (2–3 MΩ). Myocytes were suprafused at ~2 ml/min, junction potentials were corrected, and a 3-M KCl-agar bridge served as ground. Seal resistances were 5–30 GΩ, and myocytes were dialyzed for 10 min before data collection. Currents were recorded with an Axoclamp 200B and Digidata 1322A under pClamp 9 and were low-pass filtered. Successive 500-ms steps were made at 1-s intervals from −60 mV, and current-voltage (I–V) relationships were plotted from the late current. APD at 50 and 90% repolarization (APD_{50}, APD_{90}) was determined in myocytes stimulated at 1 Hz. At least 30 action potentials were recorded to verify stability, and the last 10 were averaged. Bath and pipette solutions for measuring $I_{Cl,swell}$ were designed to isolate anion currents, and those for action potentials contained physiologic anions and cations. Solution composition, preparation of reagents, and the structure of HIV PI and integrase inhibitors are given in the Online Supplement.

2.2. ROS and $\Delta\Psi_m$ measurement by flow cytometry

ROS production was detected in HL-1 myocytes loaded with C-H_2DCFDA-AM (Invitrogen), which is hydrolyzed by intracellular esterases and oxidized to fluorescent carboxy-DCF (excitation 488 nm; emission 525 nm), primarily by H_2O_2. Confluent cells were incubated with C-H_2DCFDA-AM (2.5 or 5 μM) for 30 min (37°C), washed with DPBS, and isolated by brief trypsinization. JC-1 (Invitrogen) was used to detect $\Delta\Psi_m$. HL-1 myocytes were incubate with 1 μM JC-1 for 90 min (37°C) and washed. $\Delta\Psi_m$ depolarization increases monomer (green) and decreases J-aggregate (orange-red) fluorescence (excitation: 488 nm; emission 525 and 575 nm). C-H_2DCFDA-AM and JC-1-loaded cells were assayed separately (EPICS XL; Beckman Coulter).

2.3. Statistics

Data are reported as mean ± SEM; *n* denotes number of cells (electrophysiology) or experiments (flow cytometry). One-way Repeated Measures ANOVA and the Holm-Sidak method were used ($P < 0.05$; SigmaStat 3.11). For clarity, percent block (± SEM) is sometimes reported and was calculated using each myocyte as its own control. Geometric means of fluorescence data were not normally distributed and were analyzed using Kruskal-Wallis One-way ANOVA on Ranks and Dunn's method. Non-linear fitting was done in SigmaPlot 10.1.

3. Results

3.1. Ritonavir activates $I_{Cl,swell}$

Exposure of ventricular myocytes to 15 μM RTV for 20 min activated a Cl^- current that outwardly rectified. Families of membrane currents (Fig. 1A) and corresponding I–V relationships (Fig. 1B) are shown. This outwardly rectifying current is likely to be $I_{Cl,swell}$ because it was abolished by DCPIB, a selective $I_{Cl,swell}$ blocker [26], in the presence of RTV.

RTV increased the current at +60 mV by 1.70 ± 0.16 pA/pF, from 0.42 ± 0.04 pA/pF under control conditions to 2.12 ± 0.15 pA/pF (n = 19, P <0.001) (Fig. 1C). Adding DCPIB (10 μM; 6–12 min) with RTV inhibited 95 ± 3% (n = 4, P <0.002) of RTV-induced current, and current after block was not different than control (n = 4, P = 0.71).

Activation of RTV-induced current at +60 mV was sigmoidal; latency for activation was ~3–7 min, and steady state was reached in 15–20 min. The time course for fractional activation, Y, was well-described by: $Y = 1/[1 + exp(-(t-t_{1/2})/\tau)]$, where $t_{1/2}$, the time for half-activation, was 12.0 ± 0.9 min, and τ, the time constant, was 1.8 ± 0.2 min (n = 4) (Fig. 1D). Thus, despite variable latency, activation occurred with a consistent time constant once it began.

Although RTV-induced $I_{Cl,swell}$ was readily blocked by DCPIB, stimulation of current was not easily reversed. The RTV-induced current was 1.16 ± 0.09 pA/pF and remained at 1.20 ± 0.02 pA/pF despite ~25 min of washout in control bath solution in 2 cells.

3.2. Mitochondrial ROS elicit RTV-induced $I_{Cl,swell}$

NADPH oxidase and mitochondria both generate $O_2^{-\bullet}$ that is readily dismutated to H_2O_2 spontaneously and by superoxide dismutase. Previous studies found that NADPH oxidase-dependent and exogenous H_2O_2 activate $I_{Cl,swell}$ in ventricular myocytes [19-21,25] and other cells [22-24]. The role of H_2O_2 in the RTV-induced activation of $I_{Cl,swell}$ was tested with ebselen, a membrane-permeant, glutathione peroxidase mimetic that scavenges H_2O_2. After RTV elicited $I_{Cl,swell}$, adding ebselen (15 μM, 12–20 min) in the presence of RTV blocked 105 ± 3% (n = 5, P <0.001) of RTV-induced current (Fig. 2A-C).

Next we considered the source of ROS. NADPH oxidase is a required for stretch and swelling to elicit $I_{Cl,swell}$ [19-21,25]. The role of NADPH oxidase in RTV-induced $I_{Cl,swell}$ activation was evaluated with apocynin, a selective inhibitor that prevents translocation of $p47^{phox}$ to the membrane and assembly of NADPH oxidase [27]. Apocynin (500 μM, 20 min) failed to inhibit RTV-induced current (n = 4, P = 0.98) (Fig. 3A, B). In contrast, we previously showed that apocynin effectively suppresses $I_{Cl,swell}$ elicited by swelling of cardiomyocytes [21].

Besides NADPH oxidase, mitochondria are an important source of ROS in cardiomyocytes. Complex III leaks $O_2^{-\bullet}$ to the intermembrane space from which ROS accesses the cytoplasm [28,29]. To test the role of mitochondrial ROS production, we used rotenone, a highly selective complex I inhibitor that prevents e^- transport to and ROS production by complex III. Rotenone (10 μM, 26–32 min) inhibited 100 ± 3% (n = 5, P <0.001) of RTV-induced $I_{Cl,swell}$-activation (Fig. 3C, D). Rotenone also suppresses the activation of $I_{Cl,swell}$ by antimycin A [25], which directly stimulates complex III ROS production.

3.3. Lopinavir activates $I_{Cl,swell}$ via mitochondrial ROS

RTV was not the only HIV PI that activated $I_{Cl,swell}$. As shown in Fig. 4A and B, LPV (15 μM, 20 min) increased current at +60 mV by 1.69 ± 0.14 pA/pF, from 0.81 ± 0.06 to 2.50 ± 0.16 pA/pF (n = 18, P <0.001). The magnitude of current evoked by LPV and RTV, 1.70 pA/pF (Fig. 1), were indistinguishable.

Experiments identifying the LPV-induced current as $I_{Cl,swell}$ and demonstrating that mitochondrial ROS production, rather than NADPH oxidase, was responsible are summarized in Fig. 4C. First, the $I_{Cl,swell}$ inhibitor DCPIB (10 μM, 6–12 min) blocked the LPV-induced current at +60 mV (115 ± 10%; n = 5, P <0.001) in the presence of LPV, suggesting the current was $I_{Cl,swell}$. Second, the H_2O_2 scavenger ebselen (15 μM, 12–20 min) suppressed (95 ± 5%; n = 5, P <0.001) LPV-induced current, demonstrating the involvement of ROS. Third, the NADPH oxidase inhibitor apocynin (500 μM, 20 min) failed to significant suppress LPV-induced $I_{Cl,swell}$ (8 ± 5%; n = 4, P = 0.46), implying that ROS production by NADPH oxidase

was not required. Fourth, blocking mitochondrial e^- transport with rotenone (10 μM, 26–32 min) decreased LPV-induced $I_{Cl,swell}$ by 82 ± 4% (n = 4, P <0.01). These data recapitulate the results with RTV (Fig. 1–3) and suggest that LPV and RTV modulate $I_{Cl,swell}$ by the same ROS-dependent mechanism.

3.4. Nelfinavir, amprenavir and raltegravir, an integrase inhibitor, did not block $I_{Cl,swell}$

Although both RTV and LPV activated $I_{Cl,swell}$, neither NFV (15 μM, 30 min; n = 5, P = 0.55) nor APV (15 μM, 30 min; n = 6, P = 0.11), two other HIV PI, significantly altered $I_{Cl,swell}$ within the period tested (Fig. 5). This failure to activate $I_{Cl,swell}$ was not due to the absence of the channels in the particular cells examined; hypoosmotic swelling in 0.7T elicited $I_{Cl,swell}$ in the same cells. In the NFV experiments, current at +60 mV increased from 0.89 ± 0.11 pA/pF in control to 1.44 ± 0.08 pA/pF in 0.7T (n = 5, P <0.001), and activation by 0.7T was confirmed in 2 of 2 cells challenged with APV and 0.7T (P <0.001). The HIV integrase inhibitor raltegravir (MK; 15 μM, 30 min; n = 5, P = 0.86) also failed to stimulate $I_{Cl,swell}$, whereas 0.7T elicited $I_{Cl,swell}$ in 2 of 2 cells exposed to MK and 0.7T (P <0.001).

3.5. APD

If activation of outwardly rectifying $I_{Cl,swell}$ by HIV PI is functionally significant, these agents should decrease APD in physiological solutions (Fig. 6). RTV significantly decreased APD_{50} and APD_{90} by 37 ± 7 and 60 ± 9 ms, respectively (15 μM, 15 min; n = 4), whereas APV did not alter APD (15 μM, 15 min; n = 3). Moreover, the RTV-induced reduction of APD was reversed by the $I_{Cl,swell}$ blocker DCPIB (10 μM, 10 min) in the presence of RTV. These responses are consistent with the effects of RTV, APV, and DCPIB on $I_{Cl,swell}$ and illustrate the importance of $I_{Cl,swell}$ in modulating APD. Nevertheless, RTV also reduced overshoot and plateau voltage, actions insensitive to suppression of $I_{Cl,swell}$ by DCPIB. This suggests $I_{Cl,swell}$ was not the only channel modulated by RTV, but the details were not further studied.

3.6. Mitochondrial ROS production and $\Delta\Psi_m$

To more directly assess the proposed mitochondrial ROS-dependent mechanisms of $I_{Cl,swell}$ activation, the effect of HIV PI on ROS production in HL-1 cardiomyocytes was determined by flow cytometry with C-H_2DCFDA-AM, which primarily detects H_2O_2. Fig. 7A,B display log fluorescence histograms from a single experiment. Geometric means of histograms normalized by background fluorescence are depicted in Fig. 7C. Measurements of ROS production were fully consistent with the notion that $I_{Cl,swell}$ is a ROS sensor. Both RTV and LPV (15 μM, 30 min) significantly increased ROS production 4.2-fold from background levels. This was due to mitochondrial ROS production and did not depend on NADPH oxidase. RTV- and LPV-induced ROS production was suppressed by pretreatment (30 min) with rotenone (10 μM) but was unaffected by pretreatment with the NADPH oxidase blocker gp91ds-tat (500 nM). Moreover, the HIV PI inhibitors NFV and APV and the integrase inhibitor MK failed to elicit ROS production (15 μM, 60 min). In comparison, fluorescence elicited by H_2O_2 (100 μM, 15 min) was increased 5.6-fold above background (Fig. 7A,C). Negligible responses were obtained from myocytes in the absence of fluorophore (−F) with or without addition of LPV or RTV (Fig. 7A), indicating neither myocytes nor HIV PI themselves contributed to the signal attributed to ROS. We previously demonstrated that gp91ds-tat (500 nM) fully inhibits ROS production elicited by endothelin-1, which stimulates NADPH oxidase [25].

$\Delta\Psi_m$ also was assessed in HL-1 myocytes with the potential-sensitive dye JC-1. Fig. 8 shows that RTV (15 μM, 60 min, n = 5) significantly depolarized $\Delta\Psi_m$, as reflected by the increased green:orange-red fluorescence ratio over time. After 30 min, a time when ROS production and $I_{Cl,swell}$ were augmented, the JC-1 fluorescence ratio was 2.1-fold (median) greater than control. On the other hand, APV (15 μM, 60 min, n = 4) elicited only a 20% increase at 30 min when ROS production and $I_{Cl,swell}$ were unaffected. This suggests $I_{Cl,swell}$ activation was

triggered by significant $\Delta\Psi_m$ depolarization. As a positive control, mitochondrial respiration was uncoupled with DNP (0.3 mM, 30 min, $n = 3$); this evoked a 4.5-fold increase in JC-1 fluorescence, whereas $\Delta\Psi_m$ was unchanged over 60 min in control media ($n = 3$).

Although DCPIB distinguishes between $I_{Cl,swell}$ and a number of plasmalemmal anion and cation channels [26], its mechanism and site of action are unknown. One possibility is that DCPIB blocks mitochondrial inner membrane Cl^- channel, thereby restoring $\Delta\Psi_m$ and decreasing ROS production. Rather than enhancing $\Delta\Psi_m$, DCPIB (10 μM, 10 min) increased JC-1 fluorescence in HL-1 myocytes 8.7 ± 0.9-fold ($n = 6$), indicating it strongly depolarized $\Delta\Psi_m$. In contrast, a low DCPIB concentration (0.1 μM, 10 min) that fails to suppress $I_{Cl,swell}$ increased JC-1 fluorescence by only ~20% ($n = 2$). These data suggest mitochondrial actions of DCPIB may, at least in part, explain its block $I_{Cl,swell}$.

4. Discussion

We demonstrated that certain HIV PI activate the volume-sensitive Cl^- current, $I_{Cl,swell}$, in ventricular myocytes under isosmotic conditions. At clinically relevant concentrations, RTV and LPV acutely induced an outwardly-rectifying Cl^- current, RTV decreased APD_{90} by 60 ms, and both effects were fully abolished by the $I_{Cl,swell}$-blocker DCPIB. Two other HIV PI, APV and NFV, and the HIV integrase inhibitor raltegravir (MK-0518) did not effect $I_{Cl,swell}$, and APV also did not alter APD.

Activation of $I_{Cl,swell}$ by RTV and LPV was ROS-dependent. H_2O_2 is a required intermediate in the signaling cascade regulating $I_{Cl,swell}$, and exogenous H_2O_2 activates $I_{Cl,swell}$ in rabbit ventricular myocytes [19-21,25], adenocarcinoma HeLa cells, hepatoma HTC cells, and cultured primary astrocytes [22-24]. We found RTV- and LPV-induced $I_{Cl,swell}$ was fully suppressed by the H_2O_2 scavenger ebselen. RTV and LPV augmented ROS production, as detected by C-H_2DCFDA-AM, in HL-1 myocytes, whereas APV and NFV failed to generate significant ROS after 1 h. Dichlorofluoresceins, such as C-H_2DCFDA-AM, are nominally H_2O_2-selective, but $ONOO^{-\bullet}$, HOCl, and peroxides also can contribute to its fluorescence [30]. Measurements of $\Delta\Psi_m$ with JC-1 in HL-1 myocytes suggest that RTV elicited mitochondrial ROS production, at least in part, by depolarizing $\Delta\Psi_m$. ROS and $\Delta\Psi_m$ measurements were made in HL-1 myocytes rather than acutely dissociated adult myocytes to avoid inclusion of cells damaged during isolation. Other studies confirm that $I_{Cl,swell}$ is activated by a number of the same mechanisms in HL-1 cells as in adult myocytes [31].

The two major sources of H_2O_2 in cardiomyocytes are sarcolemmal NADPH oxidase and mitochondria. These systems generate $O_2^{-\bullet}$, which is readily dismutated to H_2O_2 spontaneously and by superoxide dismutase. Previously we showed that NADPH oxidase is essential for the activation of $I_{Cl,swell}$ by β1-integrin stretch and osmotic swelling and that $I_{Cl,swell}$ can be blocked by selectively inhibiting NADPH oxidase with apocynin or gp91ds-tat [19-21,25]. However, apocynin failed to suppress the RTV-and LPV-induced currents, and pretreatment with gp91ds-tat failed to suppress C-H_2DCFDA-AM fluorescence. These data are consistent with the notion that activation of $I_{Cl,swell}$ by HIV PI was independent of NADPH oxidase.

Complex I and Complex III are the major mitochondrial redox centers that leak single e^- to molecular O_2 to generate $O_2^{-\bullet}$ [28,29]. Normally $O_2^{-\bullet}$ generated by complex I is exclusively released into the matrix of intact mitochondria and degraded by the matrix anti-oxidant system [32]. By contrast, Complex III releases $O_2^{-\bullet}$ to both sides of the mitochondrial inner membrane and accounts for extra-mitochondrial release of $O_2^{-\bullet}$ [28,32]. We propose that HIV PI elicit $I_{Cl,swell}$ via mitochondrial ROS production by Complex III. RTV- and LPV-induced $I_{Cl,swell}$ were completely abolished by rotenone, a selective Complex I inhibitor that limits downstream

e^- flux to Complex III and, therefore, inhibits mitochondrial ROS generation [28]. In addition, a 1-hr pretreatment with rotenone fully abrogated RTV- and LPV-induced H_2O_2 production measured directly by flow cytometry. Although we favor H_2O_2 as the active species, we cannot rule out the possibility that the activation of $I_{Cl,swell}$ by HIV PI involves other ROS derived from $O_2^{-\bullet}$ or H_2O_2.

A mitochondrial ROS-dependent mechanism for the activation of $I_{Cl,swell}$ is consistent with previous work showing that HIV PI reduce mitochondrial membrane potential and increases leak of e^- from the transport chain to O_2 to produce $O_2^{-\bullet}$ [11,15]. It also is consistent with our previous studies showing that blocking mitochondrial ROS production inhibits activation of $I_{Cl,swell}$ by endothelin-1 [31]. We did not evaluate whether mitochondrial ROS-induced ROS release [33] contributed to the response to HIV PI.

Despite the failure of APV and NFV to modulate $I_{Cl,swell}$ in 30 min or elicit ROS production after 1 h, it remains possible that these HIV PI also would activate cardiac $I_{Cl,swell}$ with chronic administration. APV and NFV have been shown to elicit ROS production in endothelial cells [9,34,35], vascular smooth muscle cells [10], macrophages [14], adipocytes [13,36], fibroblasts [16], and pancreatic β cells [17]. Prolonged exposures to HIV PI often employed to detect oxidative stress cannot be replicated in patch clamp studies using each myocyte as its own control.

DCPIB is regarded as a highly selective $I_{Cl,swell}$ blocker because it suppresses $I_{Cl,swell}$ without affecting several other plasmalemma Cl^-, Na^+, Ca^{2+} and K^+ channels [26], but evidence that it binds directly to $I_{Cl,swell}$ channels is lacking. Studies with JC-1 indicated that DCPIB very strongly depolarized $\Delta\Psi_m$. This raises the possibility that DCPIB uncouples mitochondrial e^- transport and blocks ROS production, which may in part explain how DCPIB inhibits $I_{Cl,swell}$. Nevertheless, DCPIB also suppresses $I_{Cl,swell}$ evoked by 100-μM exogenous H_2O_2 [32], suggesting a mitochondria-independent effect. Although DCPIB is useful to distinguish between ion channels, fully understanding its actions on mitochondrial function and the mechanism of $I_{Cl,swell}$ blockade requires additional investigation.

4.1. Potential Implications

Adverse cardiovascular effects of HIV PI include coronary artery disease and myocardial infarction [37,38], and certain HIV PI are associated with QT interval prolongation and torsade de pointes [2,4]. Anson et al. [2] demonstrated that RTV, LPV, NFV, and saquinavir substantially suppress HERG currents expressed in HEK293 cells and the corresponding endogenous current, I_{Kr}, in mouse neonatal myocytes. Block of HERG favors APD prolongation, early afterdepolarizations, and torsade de pointes [39]. Because $I_{Cl,swell}$ produces an outward current near the plateau potential, its activation favors reduction of APD. Consequently, HIV PI-induced $I_{Cl,swell}$ would antagonize APD prolongation due to block of HERG and thereby reduce the risk of drug-induced long QT syndrome and torsade de pointes. On the other hand, APD abbreviation will favor reentrant arrhythmias, such as atrial fibrillation, but an association between HIV PI and reentrant arrhythmias has not been documented. Although the present acute studies on isolated cardiomyocytes from normal animals raise important several questions, they are not sufficient to establish the role of $I_{Cl,swell}$ in HIV-infected patients who are treated with HIV PI as part of multidrug highly active anti-retroviral therapy.

Although several mechanisms underlying the untoward effects of HIV PI have been the focus of research, the potential role of ion channels in these outcomes largely has been ignored. Because $I_{Cl,swell}$ is present in a number of tissues affected by HIV PI, such as macrophages, hepatocytes, endothelial cells, and pancreatic β cells, it is reasonable to consider whether $I_{Cl,swell}$ activation might contribute to the untoward effects of HIV PI. HIV PI-induced ROS

production also may regulate other redox sensitive ion channels and transporters that are widely distributed. Na channels [40], L-type Ca^{2+} channels, transient outward K^+ channels, inwardly rectifying K^+ channels, ATP-sensitive K^+ channels, ryanodine receptors, inositol-1,4,5-trisphosphate receptors, sarcoplasmic reticulum and plasma membrane Ca^{2+} ATPases, and the Na^+–Ca^{2+} exchanger [41] are influenced by ROS. Whether HIV PI modulate these channels and transporters and whether they contribute to the adverse effects of HIV PI in heart and other systems remains to be elucidated.

Supplementary Material

Refer to Web version on PubMed Central for supplementary material.

Acknowledgments

We thank Frances K. H. White and Julie Farnsworth for training and assistance in flow cytometry. Supported by grants from the American Heart Assoc. (0855044E), NIH (R01AT004148, R21AI068432, R01AI057189), and by the Massey Cancer Center Flow Cytometry & Imaging Shared Resource Facility (P30CA16059).

References

1. Flint OP, Noor MA, Hruz PW, Hylemon PB, Yarasheski K, Kotler DP, et al. The role of protease inhibitors in the pathogenesis of HIV-associated lipodystrophy: cellular mechanisms and clinical implications. Toxicol Pathol 2009;37:65–77. [PubMed: 19171928]
2. Anson BD, Weaver JG, Ackerman MJ, Akinsete O, Henry K, January CT, et al. Blockade of HERG channels by HIV protease inhibitors. Lancet 2005;365:682–6. [PubMed: 15721475]
3. Busti AJ, Tsikouris JP, Peeters MJ, Das SR, Canham RM, Abdullah SM, et al. A prospective evaluation of the effect of atazanavir on the QTc interval and QTc dispersion in HIV-positive patients. HIV Med 2006;7:317–22. [PubMed: 16945077]
4. Chinello P, Lisena FP, Angeletti C, Boumis E, Papetti F, Petrosillo N. Role of antiretroviral treatment in prolonging QTc interval in HIV-positive patients. J Infect 2007;54:597–602. [PubMed: 17174400]
5. Fiala M, Murphy T, MacDougall J, Yang W, Luque A, Iruela-Arispe L, et al. HAART drugs induce mitochondrial damage and intercellular gaps and gp120 causes apoptosis. Cardiovasc Toxicol 2004;4:327–37. [PubMed: 15531776]
6. Hruz PW, Yan Q, Struthers H, Jay PY. HIV protease inhibitors that block GLUT4 precipitate acute, decompensated heart failure in a mouse model of dilated cardiomyopathy. FASEB J 2008;22:2161–7. [PubMed: 18256305]
7. McArthur MA, Kalu SU, Foulks AR, Aly AM, Jain SK, Patel JA. Twin preterm neonates with cardiac toxicity related to lopinavir/ritonavir therapy. Pediatr Infect Dis J 2009;28:1127–9. [PubMed: 19820426]
8. Conklin BS, Fu W, Lin PH, Lumsden AB, Yao Q, Chen C. HIV protease inhibitor ritonavir decreases endothelium-dependent vasorelaxation and increases superoxide in porcine arteries. Cardiovasc Res 2004;63:168–75. [PubMed: 15194474]
9. Chai H, Yang H, Yan S, Li M, Lin PH, Lumsden AB, et al. Effects of 5 HIV protease inhibitors on vasomotor function and superoxide anion production in porcine coronary arteries. J Acquir Immune Defic Syndr 2005;40:12–9. [PubMed: 16123675]
10. Rudich A, Ben-Romano R, Etzion S, Bashan N. Cellular mechanisms of insulin resistance, lipodystrophy and atherosclerosis induced by HIV protease inhibitors. Acta Physiol Scand 2005;183:75–88. [PubMed: 15654921]
11. Jiang B, Hebert VY, Li Y, Mathis JM, Alexander JS, Dugas TR. HIV antiretroviral drug combination induces endothelial mitochondrial dysfunction and reactive oxygen species production, but not apoptosis. Toxicol Appl Pharmacol 2007;224:60–71. [PubMed: 17669453]
12. Wang X, Chai H, Lin PH, Yao Q, Chen C. Roles and mechanisms of human immunodeficiency virus protease inhibitor ritonavir and other anti-human immunodeficiency virus drugs in endothelial dysfunction of porcine pulmonary arteries and human pulmonary artery endothelial cells. Am J Pathol 2009;174:771–81. [PubMed: 19218343]

13. Ben-Romano R, Rudich A, Etzion S, Potashnik R, Kagan E, Greenbaum U, et al. Nelfinavir induces adipocyte insulin resistance through the induction of oxidative stress: differential protective effect of antioxidant agents. Antivir Ther 2006;11:1051–60. [PubMed: 17302375]
14. Lagathu C, Eustace B, Prot M, Frantz D, Gu Y, Bastard JP, et al. Some HIV antiretrovirals increase oxidative stress and alter chemokine, cytokine or adiponectin production in human adipocytes and macrophages. Antivir Ther 2007;12:489–500. [PubMed: 17668557]
15. Wang X, Mu H, Chai H, Liao D, Yao Q, Chen C. Human immunodeficiency virus protease inhibitor ritonavir inhibits cholesterol efflux from human macrophage-derived foam cells. Am J Pathol 2007;171:304–14. [PubMed: 17591975]
16. Caron M, Auclair M, Donadille B, Bereziat V, Guerci B, Laville M, et al. Human lipodystrophies linked to mutations in A-type lamins and to HIV protease inhibitor therapy are both associated with prelamin A accumulation, oxidative stress and premature cellular senescence. Cell Death Differ 2007;14:1759–67. [PubMed: 17612587]
17. Chandra S, Mondal D, Agrawal KC. HIV-1 Protease Inhibitor Induced Oxidative Stress Suppresses Glucose Stimulated Insulin Release: Protection with Thymoquinone. Exp Biol Med (Maywood) 2009;234:442–53. [PubMed: 19234050]
18. Viengchareun S, Caron M, Auclair M, Kim MJ, Frachon P, Capeau J, et al. Mitochondrial toxicity of indinavir, stavudine and zidovudine involves multiple cellular targets in white and brown adipocytes. Antivir Ther 2007;12:919–29. [PubMed: 17926646]
19. Browe DM, Baumgarten CM. Angiotensin II (AT1) receptors and NADPH oxidase regulate Cl^- current elicited by β1 integrin stretch in rabbit ventricular myocytes. J Gen Physiol 2004;124:273–87. [PubMed: 15337822]
20. Browe DM, Baumgarten CM. EGFR kinase regulates volume-sensitive chloride current elicited by integrin stretch via PI-3K and NADPH oxidase in ventricular myocytes. J Gen Physiol 2006;127:237–51. [PubMed: 16505146]
21. Ren Z, Raucci FJ Jr, Browe DM, Baumgarten CM. Regulation of swelling-activated Cl current by angiotensin II signalling and NADPH oxidase in rabbit ventricle. Cardiovasc Res 2008;77:73–80. [PubMed: 18006461]
22. Varela D, Simon F, Riveros A, Jorgensen F, Stutzin A. NAD(P)H oxidase-derived H_2O_2 signals chloride channel activation in cell volume regulation and cell proliferation. J Biol Chem 2004;279:13301–4. [PubMed: 14761962]
23. Shimizu T, Numata T, Okada Y. A role of reactive oxygen species in apoptotic activation of volume-sensitive Cl^- channel. Proc Natl Acad Sci U S A 2004;101:6770–3. [PubMed: 15096609]
24. Haskew-Layton RE, Mongin AA, Kimelberg HK. Hydrogen peroxide potentiates volume-sensitive excitatory amino acid release via a mechanism involving Ca^{2+}/calmodulin-dependent protein kinase II. J Biol Chem 2005;280:3548–54. [PubMed: 15569671]
25. Deng W, Baki L, Baumgarten CM. Endothelin signaling regulates volume-sensitive Cl current via NADPH oxidase and mitochondrial reactive oxygen species. Cardiovasc Res. 2010 Epub ahead of print. 10.1093/cvr/cvq125
26. Decher N, Lang HJ, Nilius B, Bruggemann A, Busch AE, Steinmeyer K. DCPIB is a novel selective blocker of $I_{Cl,swell}$ and prevents swelling-induced shortening of guinea-pig action potential duration. Br J Pharmacol 2001;134:1467–79. [PubMed: 11724753]
27. Ximenes VF, Kanegae MP, Rissato SR, Galhiane MS. The oxidation of apocynin catalyzed by myeloperoxidase: proposal for NADPH oxidase inhibition. Arch Biochem Biophys 2007;457:134–41. [PubMed: 17166480]
28. Chen Q, Vazquez EJ, Moghaddas S, Hoppel CL, Lesnefsky EJ. Production of reactive oxygen species by mitochondria: central role of complex III. J Biol Chem 2003;278:36027–31. [PubMed: 12840017]
29. Turrens JF. Mitochondrial formation of reactive oxygen species. J Physiol 2003;552:335–44. [PubMed: 14561818]
30. Tarpey MM, Wink DA, Grisham MB. Methods for detection of reactive metabolites of oxygen and nitrogen: in vitro and in vivo considerations. Am J Physiol Regul Integr Comp Physiol 2004;286:R431–R444. [PubMed: 14761864]
31. Deng W, Raucci FJ Jr, Baki L, Baumgarten CM. Regulation of volume-sensitive chloride current in cardiac HL-1 myocytes. Biophys J 2010;98(Suppl 1):338a.

32. Muller FL, Liu Y, Van RH. Complex III releases superoxide to both sides of the inner mitochondrial membrane. J Biol Chem 2004;279:49064–73. [PubMed: 15317809]
33. Aon MA, Cortassa S, Marban E, O'Rourke B. Synchronized whole cell oscillations in mitochondrial metabolism triggered by a local release of reactive oxygen species in cardiac myocytes. J Biol Chem 2003;278:44735–44. [PubMed: 12930841]
34. Mondal D, Pradhan L, Ali M, Agrawal KC. HAART drugs induce oxidative stress in human endothelial cells and increase endothelial recruitment of mononuclear cells: exacerbation by inflammatory cytokines and amelioration by antioxidants. Cardiovasc Toxicol 2004;4:287–302. [PubMed: 15470276]
35. Grigorian A, Hurford R, Chao Y, Patrick C, Langford TD. Alterations in the Notch4 pathway in cerebral endothelial cells by the HIV aspartyl protease inhibitor, nelfinavir. BMC Neurosci 2008;9:27. [PubMed: 18302767]
36. Vincent S, Tourniaire F, El Yazidi CM, Compe E, Manches O, Plannels R, et al. Nelfinavir induces necrosis of 3T3F44-2A adipocytes by oxidative stress. J Acquir Immune Defic Syndr 2004;37:1556–62. [PubMed: 15577407]
37. Lekakis J, Tsiodras S, Ikonomidis I, Palios J, Poulakou G, Rallidis L, et al. HIV-positive patients treated with protease inhibitors have vascular changes resembling those observed in atherosclerotic cardiovascular disease. Clin Sci (Lond) 2008;115:189–96. [PubMed: 18251713]
38. Vaughn G, Detels R. Protease inhibitors and cardiovascular disease: analysis of the Los Angeles County adult spectrum of disease cohort. AIDS Care 2007;19:492–9. [PubMed: 17453589]
39. Roden DM. Cellular basis of drug-induced torsades de pointes. Br J Pharmacol 2008;154:1502–7. [PubMed: 18552874]
40. Song Y, Shryock JC, Wagner S, Maier LS, Belardinelli L. Blocking late sodium current reduces hydrogen peroxide-induced arrhythmogenic activity and contractile dysfunction. J Pharmacol Exp Ther 2006;318:214–22. [PubMed: 16565163]
41. Zima AV, Blatter LA. Redox regulation of cardiac calcium channels and transporters. Cardiovasc Res 2006;71:310–21. [PubMed: 16581043]

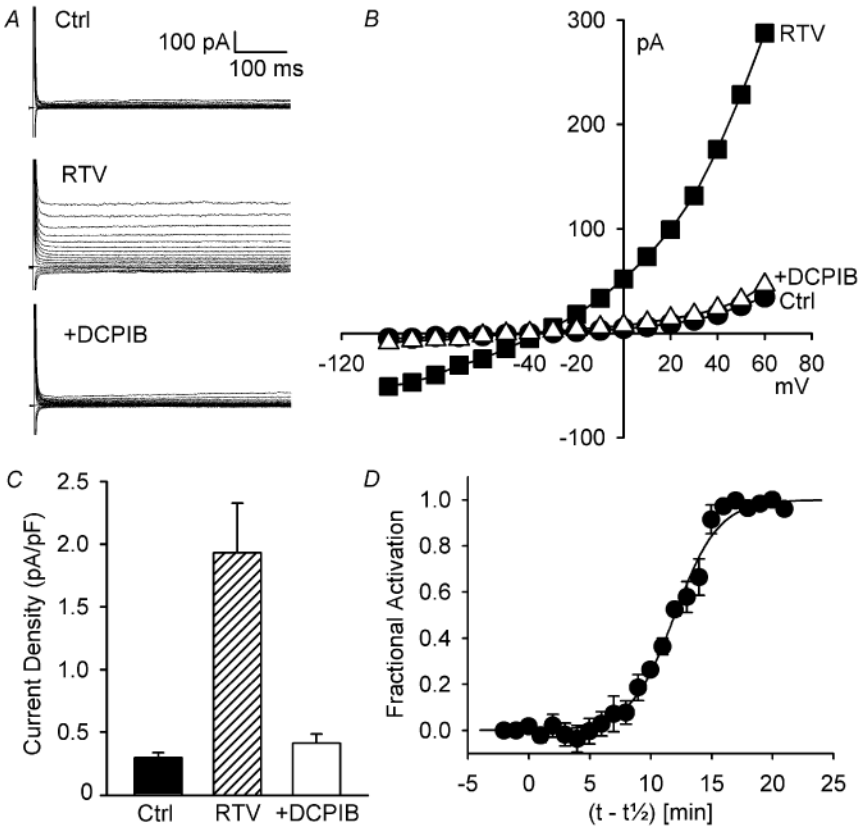

Fig. 1.

Ritonavir (RTV) activated volume-sensitive Cl^- current ($I_{Cl,swell}$) under isosmotic conditions; RTV-induced currents outwardly rectified and were blocked by DCPIB. (A) Families of currents (-100 to + 60 mV, 500 ms) in control (Ctrl), after RTV exposure (15 μM, 20 min), and after addition of DCPIB (10 μM, 6 min) in presence of RTV (+DCPIB). (B) I-V relationships from A. (C) Current densities at +60 mV (n = 4; Ctrl vs. RTV, P <0.002; RTV vs. +DCPIB, P <0.002; Ctrl vs. +DCPIB, P = 0.71). (D) Kinetics of activation of $I_{Cl,swell}$ by RTV (n = 4).

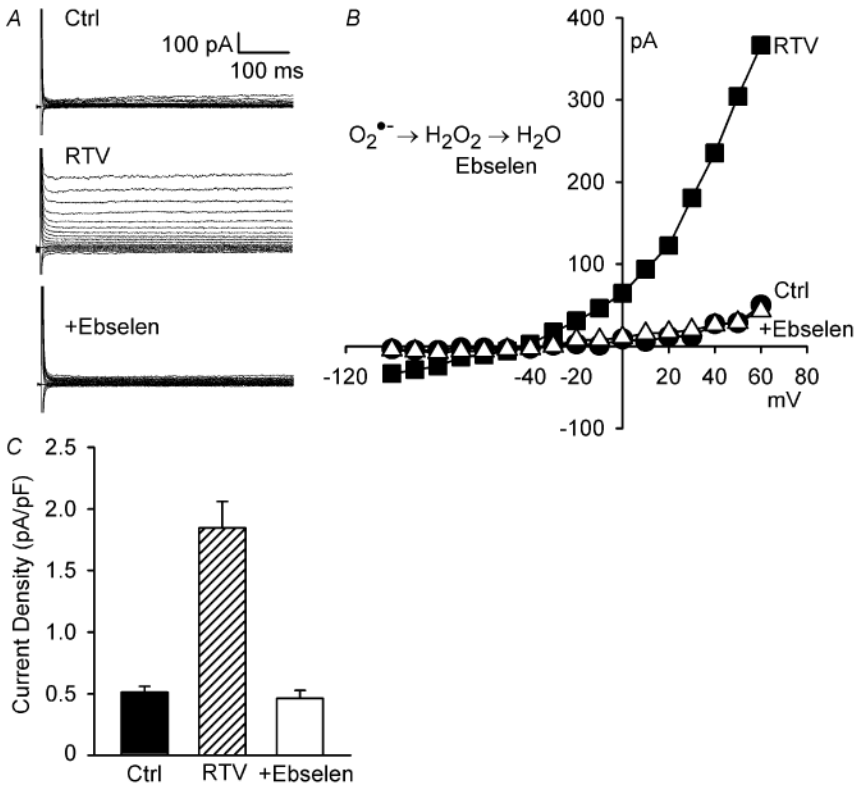

Fig. 2.

RTV-induced activation of $I_{Cl,swell}$ was reversed by ebselen, a H_2O_2 scavenger. (A) Currents in control (Ctrl), after RTV exposure (15 μM, 20 min), and after addition of ebselen (15 μM, 15 min) in presence of RTV. (B) I-V relationships from A. (C) Current densities at +60 mV (n = 5; Ctrl vs. RTV, P <0.001; RTV vs. +Ebselen, P <0.001; Ctrl vs. +Ebselen, P = 0.81).

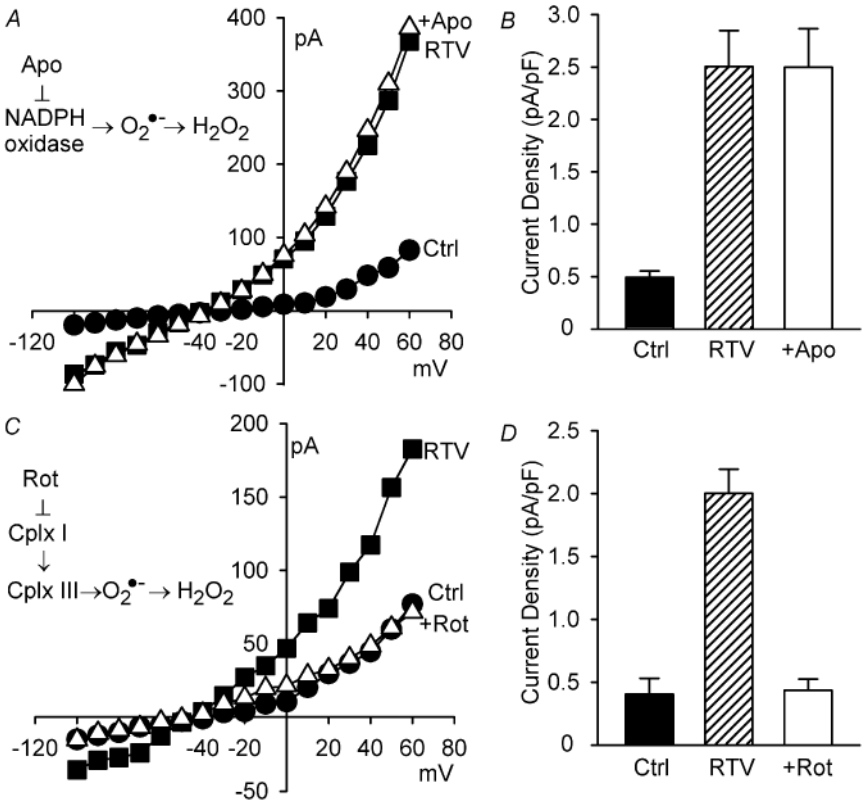

Fig. 3.

RTV elicited $I_{Cl,swell}$ via ROS from mitochondria but not NADPH oxidase. (A, B) Apocynin (Apo; 500 μM, 20 min), a specific NADPH oxidase inhibitor, failed to suppress RTV (15 μM, 20 min)-induced $I_{Cl,swell}$ (n = 4; Ctrl vs. RTV, P <0.001; RTV vs. +Apo, P = 0.98; Ctrl vs. +Apo, P <0.001). (C, D) In contrast, rotenone (Rot; 10 μM, 30 min), which suppresses mitochondrial ROS production, fully inhibited RTV-induced $I_{Cl,swell}$ (n = 5; Ctrl vs. RTV, P <0.001; RTV vs. +Rot, P <0.001; Ctrl vs. +Rot, P = 0.89).

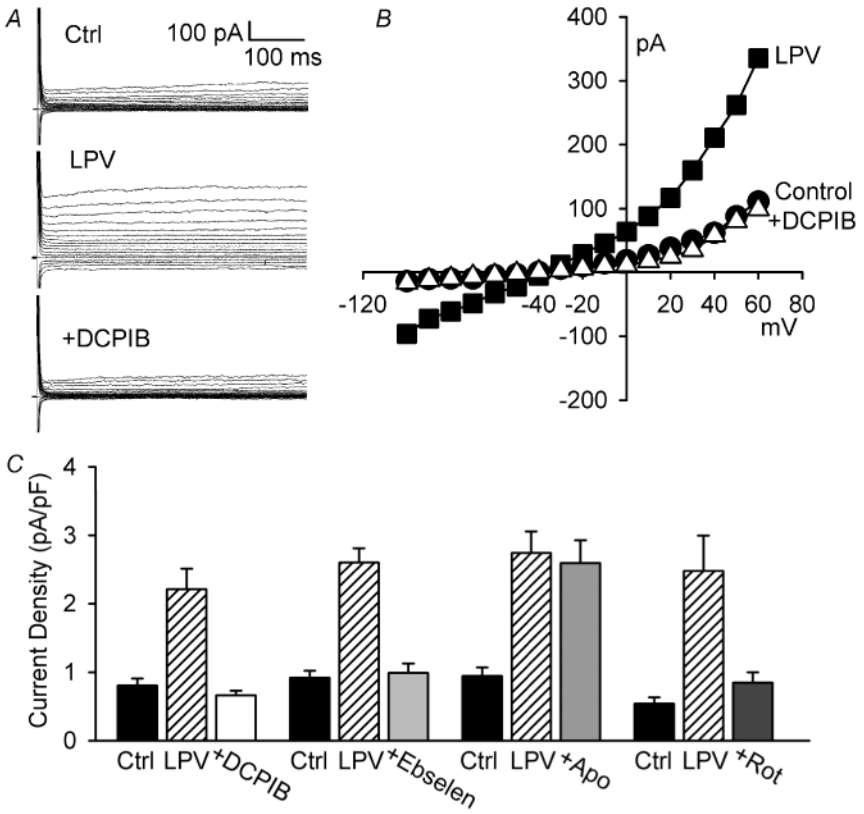

Fig. 4.

Lopinavir (LPV) activated $I_{Cl,swell}$ via mitochondrial ROS production but not NADPH oxidase. (A, B) LPV (15 μM, 25 min) elicited outwardly rectifying Cl^- current that was completely blocked by DCPIB. (C) Current densities at +60 mV showing block of LPV-induced current by DCPIB (n = 5, Ctrl vs. LPV, P <0.001; LPV vs. +DCPIB, P <0.001; Ctrl vs. +DCPIB, P = 0.55), ebselen (n = 5, Ctrl vs. LPV, P <0.001; LPV vs. +Ebselen, P <0.001; Ctrl vs. +Ebselen, P = 0.72), and rotenone (n = 4, Ctrl vs. LPV, P <0.003; LPV vs. +Rot, P <0.006; Ctrl vs. +Rot, P = 0.45). In contrast, LPV-induced current was unaffected by apocynin (n = 4, Ctrl vs. LPV, P <0.001; LPV vs. +Apo, P = 0.79; Ctrl vs. +Apo, P <0.001).

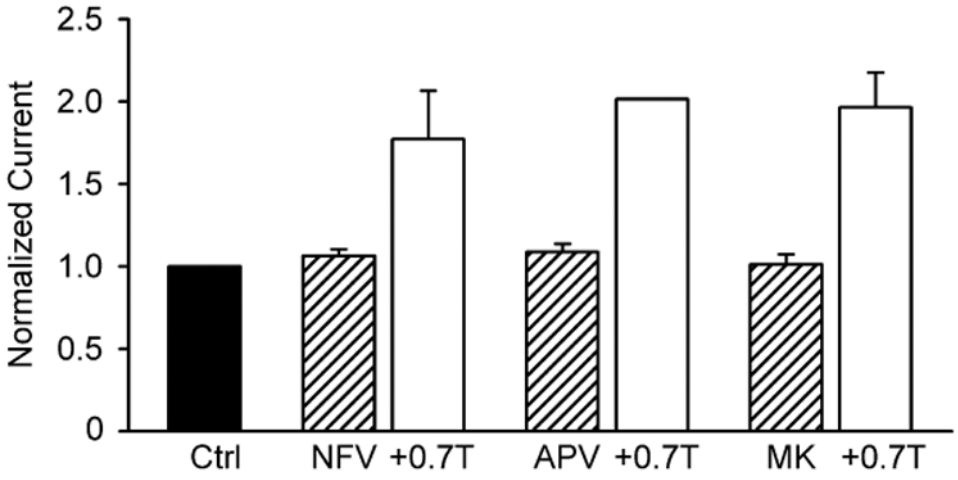

Fig. 5.

The HIV PI nelfinavir (NFV; 5 μM, 30 min; *n* = 5) and amprenavir (APV; 15 μM, 30 min, *n* = 6) and the HIV integrase inhibitor raltegravir (MK; 15 μM, 30 min, *n* = 5) failed to activate $I_{Cl,swell}$ acutely. By contrast, $I_{Cl,swell}$ was elicited by osmotic swelling in 0.7T bath solution in the continued presence of HIV protease or integrase inhibitors (for drug + 0.7T, *n* = 5, 2 and 2, respectively). Currents were normalized to Ctrl for each experimental group.

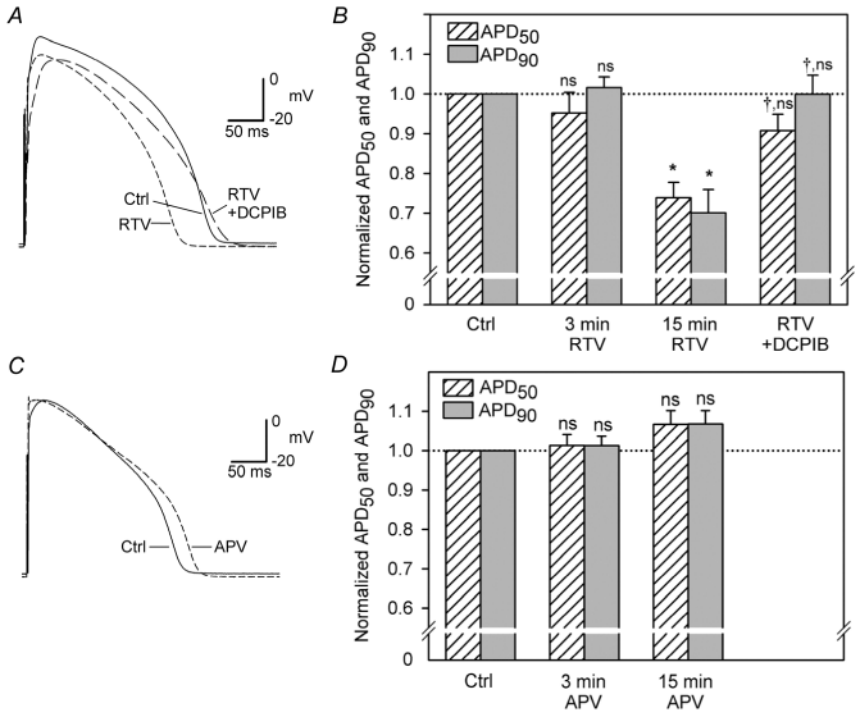

Fig. 6.

Effects of RTV and APV on ventricular action potentials and normalized APD_{50} and APD_{90}. (A,B) RTV (15 μM, 15 min; $n = 4$) significantly decreased APD_{50} and APD_{90}, and abbreviation of APD was reversed by DCPIB (10 μM, 10 min). *, $P < 0.05$ vs Ctrl; †, vs 15 min RTV; ns, vs Ctrl. (C,D) APV (15 μM, 15 min; $n = 3$) did not significantly alter APD; ns, vs Ctrl.

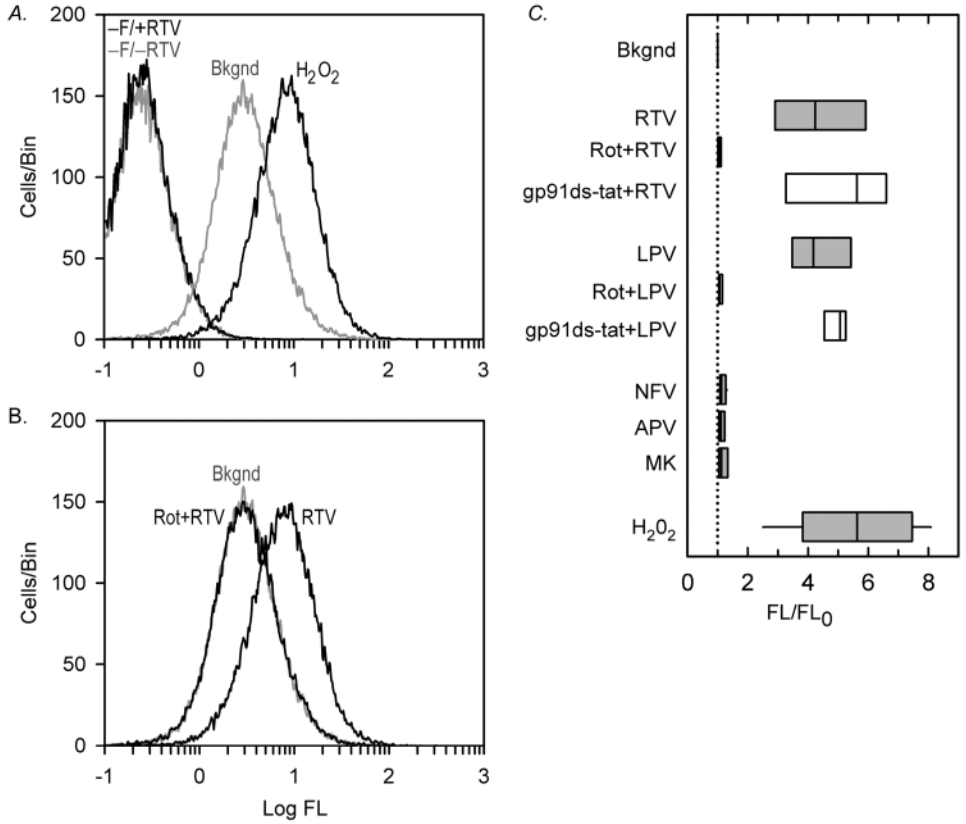

Fig. 7.

RTV- and LPV-induced mitochondrial ROS production in HL-1 myocytes. (A) Log fluorescence (FL) histograms by flow cytometry. Negative controls in absence of probe (−F) without (−RTV) or with (+RTV) RTV (15 μM, 30 min). In fluorophore-loaded myocytes, background fluorescence (Bkgnd) and response to H_2O_2 (100 μM, 15 min) reflect ROS. (B) RTV elicited ROS production, and pretreatment with rotenone (10 μM, 30 min; Rot+RTV) suppressed ROS to background levels; A and B, from same experiment. (C) Geometric means of histograms normalized by background fluorescence (FL/FL_O). Both RTV and LPV (15 μM, 30 min; $n = 5$, for each) significantly increased ROS production, which was fully suppressed by pretreatment with Rot (10 μM, 30 min; $n = 5$, for each) but not by pretreatment with gp91ds-tat (500 nM, 30 min; $n = 3$, for each). In contrast, NFV ($n = 4$), APV ($n = 3$), and MK ($n = 3$; 15 μM, 60 min, for each) failed to augment ROS production. H_2O_2 (100 μM, 15 min; $n = 9$) was positive control. Box plots show 25, 50 and 75%ile, and whiskers show 5 and 95%ile; dotted line, background fluorescence.

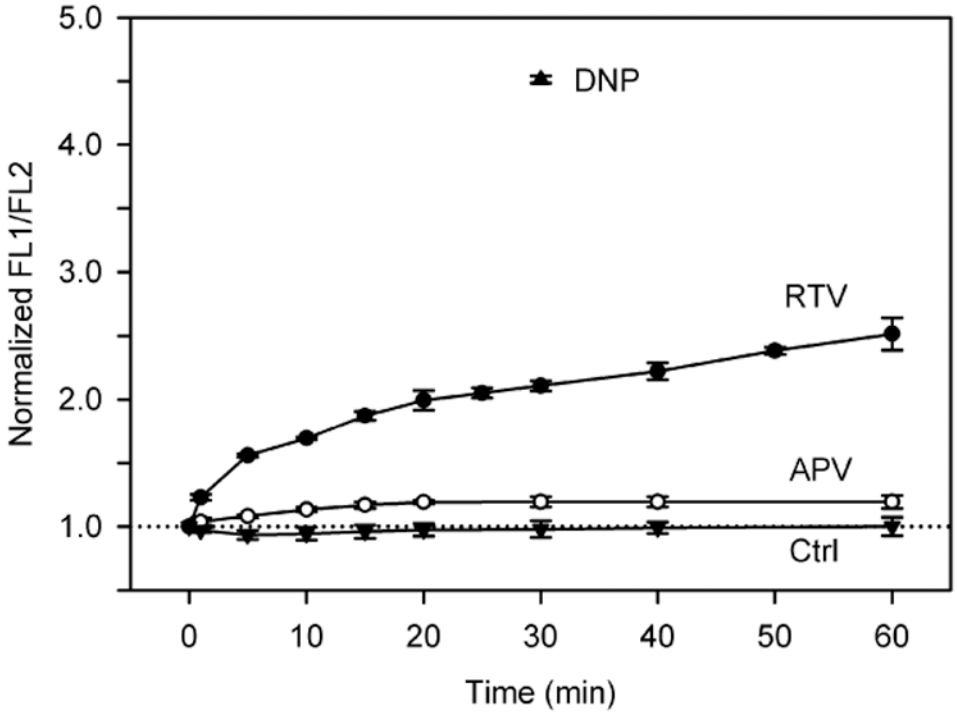

Fig. 8.

Time-dependence of RTV-induced $\Delta\Psi_m$ depolarization in HL-1 myocytes. Ratios of JC-1 fluorescence (FL1/FL2) normalized by control fluorescence ratio are plotted for RTV (15 μM; $n = 5$), APV (15 μM; $n = 4$), and a time control (Ctrl; $n = 3$). Treatment with DNP (0.3 mM, 20 min) served as positive control. Increased FL1/FL2 corresponds to depolarization of $\Delta\Psi_m$.